Electronic Supplementary Material (ESI) for Green Chemistry.
This journal is © The Royal Society of Chemistry 2014

Supporting Information

Environmentally-friendly high-energy MOFs: crystal structure, thermostability, insensitivity and remarkable detonation performance

Xiangyu Liu,[a, b #] Wenjuan Gao,[a #] Panpan Sun,[a] Zhiyong Su,[a] Sanping Chen, *[a] Qing Wei,[a] Gang Xie,[a] and Shengli Gao[a]

[a] Key Laboratory of Synthetic and Natural Functional Molecule Chemistry of Ministry of Education, College of Chemistry and Materials Science, Northwest University, Xi'an 710069, China

[b] School of Chemistry and Chemical Engineering, Ningxia University, Yinchuan 750021, China

[#] These authors have equal contribution to this work.

***Corresponding author**

Prof. Sanping Chen

Tel.: +86-029-88302604

Fax: +86-029-88302604

E-mail: sanpingchen@126.com

Table of contents

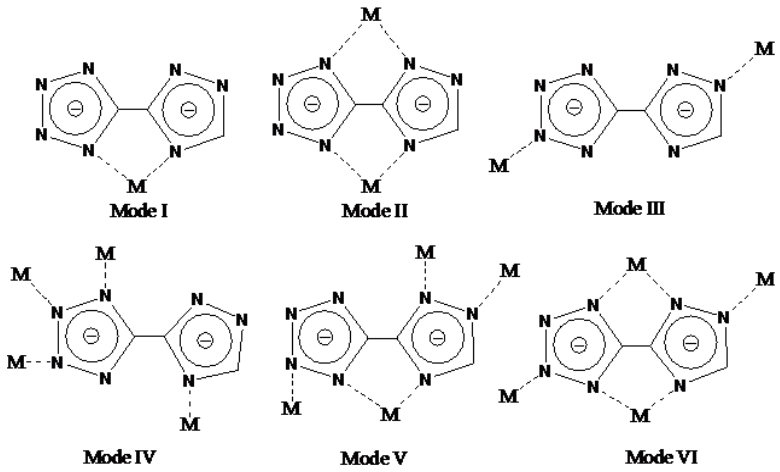

Scheme S1. Coordination Modes of 3-(1*H*-tetrazol-5-yl)-1*H*-triazole ligand.

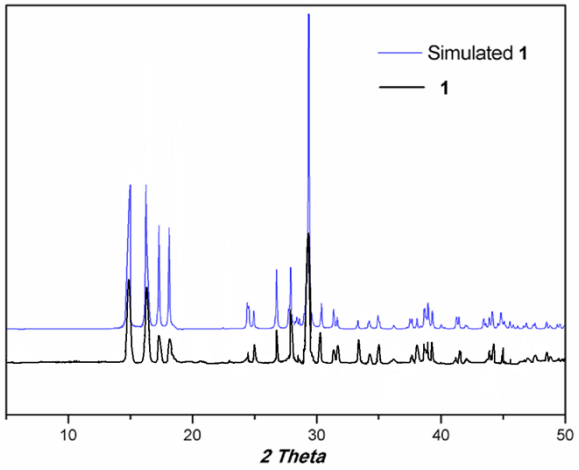

Figure S1. X-ray powder diffraction (XRPD) curves of **1**.

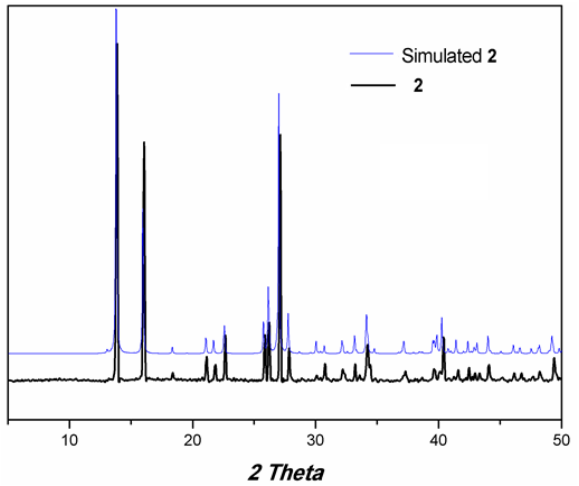

Figure S2. XRPD curves of **2**.

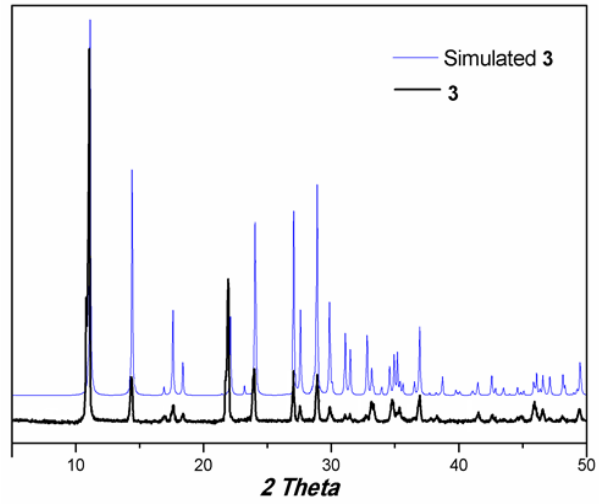

Figure S3. XRPD curves of **3**.

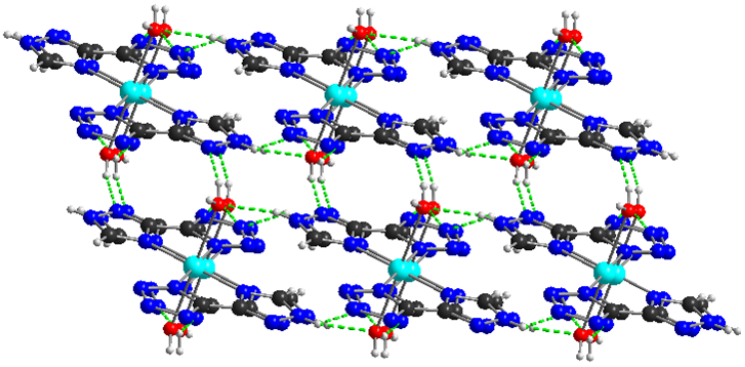

Figure S4. 3D supramolecular network in **1**. (Hydrogen atoms are omitted for clarity)

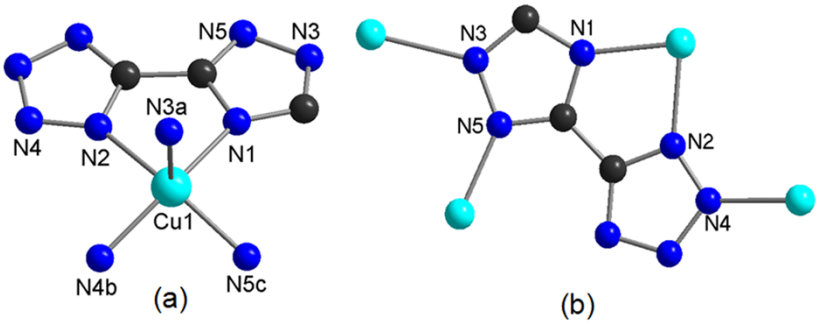

Figure S5. (a) Coordination environment of Cu(II) ions in **2**. (b) Coordination mode of tztr ligand in **2**. (Hydrogen atoms are omitted for clarity)

1. Materials and instruments

All the materials and reagents were obtained commercially and used without further purifications. Elemental analyses (C, H and N) were carried on a Vario EL III analyzer fully automated trace element analyzer and IR spectra of complexes were measured on a Bruker FTIR with KBr pellets. The valence states of Cu ions in complexes were confirmed by a Thermo ESCALAB 250Xi X-ray photoelectric spectrometer. Thermogravimetric analysis (TGA) and differential scanning calorimetry (DSC) were performed on a CDR-4P thermal analyzer of Shanghai Balance Instrument factory and a Netzsch STA 449C instrument, respectively, using dry oxygen-free nitrogen as the atmosphere with a flowing rate of 10 mL·min^{-1}. About 0.6 mg sample was sealed in aluminum pans in the temperature range of 25-500 ^{o}C for DSC experiments. Thermogravimetry-Fourier transform infrared spectrometry of the detonation products were carried out on a TG-209/Vector TM-22 instrument. The sensitivities to impact stimuli were determined by fall hammer apparatus applying standard staircase method using a 2 kg drop weight and the results were reported in terms of height for 50% probability of explosion ($h_{50\%}$).[1] The friction sensitivities were determined on a Julius Peter's apparatus by following the BAM method.[2] The electrostatic sensitivities were carried out by using an ESD JGY-50 III electric spark tester. The purity of the bulk samples were verified by X-ray powder diffraction (XRPD) measurements performed on a Rigaku RU200 diffractometer at 60 kV, 300 mA and Cu *K*α radiation (λ = 1.5406 Å), with a scan speed of 5°·min^{-1} and a step size of 0.02° in 2θ. Densities of three complexes were measured by using Automatic Density Analyzer, ULTRAPYC 1200e. 1H NMR spectra was recorded on a Varian unity INOVA-400 instrument in [D6] DMSO at 25^{o}C.

2. Synthetic procedures

General caution: H_2tztr and complexes are potentially explosive. Therefore, only small amounts of complexes should be prepared and they should be handled with care.

3-(1*H*-tetrazol-5-yl)-1*H*-triazole. 5-cyano-1*H*-1,2,4-triazole (2.24 g, 23.9 mmol), sodium azide (1.71 g, 26.3 mmol), and zinc chloride (4.0 g, 29.3 mmol) were suspended in water (120 mL) and the reaction mixture was refluxed for 16 h. After cooling to room temperature, 2$_M$ HCl (20 mL) were added to avoid precipitation of zinc hydroxide. The precipitate was collected by filtration, washed with water, and dried in air to yield 3-(1*H*-tetrazol-5-yl)-1*H*-triazole (Yield 85%, based on

5-cyano-1H-1,2,4-triazole) as colorless solid. For $C_3H_3N_7$ (137.08): C, 26.26; H, 2.18; N, 71.49%. Found: C, 26.23; H, 2.14; N, 71.40%. ^{1}H NMR (400 MHz, [D6]DMSO, ppm): δ=8.88 (s, $H_{triazole/tetrazole}$). IR (cm^{-1}, KBr): 3453w, 3219s, 2973w, 1878m, 1616m, 1458s, 1340m, 1266s, 1224s, 1077m, 1035m, 947m, 801m, 699w, 626m, 482s.

[Cu(Htztr)$_2$(H$_2$O)$_2$]$_n$ (1). A mixture of H_2tztr (411 mg, 0.3 mmol) and $CuCl_2 \cdot 2H_2O$ (170 mg, 0.1 mmol) were dissolved in 8 mL of water and stirring at room temperature. When the pH of the mixture was adjusted to about 4.5 with ammonia solution, the solution was put into a 15 mL Teflon liner, heated to 140 °C for 50 h, and then cooled to room temperature at a rate of 5 $^oC \cdot h^{-1}$. The blue flaky crystals were obtained (Yield 56%, based on Cu). Anal. Calcd. For $CuC_6H_8N_{14}O_2$ (371.80): C, 19.36; H, 2.15; N, 52.72%. Found: C, 19.35; H, 2.13; N, 52.71%. IR (cm^{-1}, KBr): 3449s, 3169w, 2925w, 2852w, 2362w, 1736w, 1620s, 1513s, 1433s, 1354s, 1318s, 1224m, 1181s, 1088m, 1037m, 1001m, 871w, 712m, 662m, 525m, 482w. The XPS spectrum of the crystalline sample show evident satellite peaks of $^2P_{2/3}$ and $^2P_{1/2}$ at 943.3 and 962.7 eV, respectively, suggesting Cu(II) in compound **1**.

{[Cu(tztr)]·H$_2$O}$_n$ (2). Complex **2** was synthesized in the similar way as that described for **1**, except that the pH value of the mixture was adjusted to about 7.0 with ammonia solution. The green prism-shaped crystals were obtained (Yield 55%, based on Cu). Anal. Calcd. For $CuC_3H_3N_7O$ (216.65): C, 16.61; H, 1.38; N, 45.23%. Found: C, 16.60; H, 1.36; N, 45.20%. IR (cm^{-1}, KBr): 3447s, 3109w, 2925w, 2850w, 1627s, 1508s, 1429s, 1389s, 1321m, 1283w, 1224m, 1176w, 1145m, 1090m, 1007m, 868w, 770w, 708m, 665m, 536w, 473w. The XPS spectrum of the crystalline sample show the evident satellite peaks of $^2P_{2/3}$ and $^2P_{1/2}$ at 942.7 and 962.1 eV, respectively, also confirming the presence of Cu(II) in compound **2**.

[Cu(Htztr)]$_n$ (3). Complex **3** was synthesized in the similar way as that described for **1**, except replacing $CuCl_2 \cdot 2H_2O$ with CuCN and the pH value of the mixture was adjusted to about 5.5 with ammonia solution. The colorless flaky crystals were obtained (Yield 50%, based on Cu). Anal. Calcd. For $CuC_3H_2N_7$ (199.66): C, 18.02; H, 1.00; N, 49.08%. Found: C, 17.98; H, 0.98; N, 49.05%. IR (cm^{-1}, KBr): 3134s, 3075w, 2992w, 2793w, 2547w, 1814w, 1599w, 1540w, 1473s, 1388w, 1340s, 1299s, 1100m, 1024w, 990w, 883m, 767w, 743m, 637m, 426s. The XPS spectrum of the crystalline sample show the shoulder peaks at 934.3 and 954 eV, respectively, indicating that compound **3** contains Cu(I) ions.

3. X-ray crystallography determinations

The single crystal X-ray experiments were performed on a Bruker Smart Apex CCD diffractometer equipped with graphite monochromatized Mo *K*α radiation (λ = 0.71073 Å) using ω and φ scan mode. The single-crystal structures were solved by direct methods using SHELXS-97[3] and refined by means of full-matrix least-squares procedures on F^2 with SHELXL-97[4] program. All non-H atoms were located using subsequent Fourier-difference methods and refined anisotropically. In all cases, hydrogen atoms were placed in calculated positions and thereafter allowed to ride on their parent atoms. Experimental details for the structural determination of complexes are summarized in Table S1 while the selected bond lengths and angles data are presented in Table S2. Hydrogen bonding parameters are listed in Table S3.

Table S1. Crystal data and structure refinement details for three complexes.

	1	**2**	**3**
Empirical formula	$CuC_6H_8N_{14}O_2$	$CuC_3H_3N_7O$	$CuC_3H_2N_7$
Formula weight	371.81	216.65	199.67
Crystal system	Triclinic	Monoclinic	Monoclinic
space group	$P\bar{1}$	*P*2(1)/*n*	*P*2(1)/*n*
a (Å)	7.1861(14)	7.404(3)	8.630(3)
b (Å)	7.5759(14)	9.672(3)	9.867(3)
c (Å)	7.6549(14)	9.341(3)	6.736(2)
α (°)	89.212(4)	90	90
β (°)	63.414(3)	113.020	108.297
γ (°)	64.027(3)	90	90
V (Å^3)	326.32(11)	615.7(4)	544.6(3)
Z	1	4	4
D_c (g·cm^{-3})	1.892	2.316	2.435
T (K)	293(2)	296(2)	296(2)
μ (mm^{-1})	1.714	3.499	3.932
F(000)	187	420	392
R_{int}	0.0275	0.0610	0.0482
Goodness of fit (F^2)	0.953	1.104	1.008
Reflections collected/unique	1974 / 1449	3338 / 1313	986 / 695
R(int)	0.0275	0.0610	0.0691
R_1 [a] [$I>2\sigma(I)$]	0.0586	0.0837	0.0775
wR_2 [b] (all data)	0.1641	0.2321	0.1993

[a] $R_1 = \sum||F_o|-|F_c||/\sum|F_o|$; [b] $wR_2 = [\sum w(F_o^2-F_c^2)^2/\sum w[(F_o^2)^2]]^{1/2}$.

Table S2. Selected bond lengths (Å) and bond angles (°) for the complexes.

Complex **1**

N(4)-Cu(1)#1	1.995(7)	N(6)-N(4)-Cu(1)#1	125.0(6)
N(3)-Cu(1)#2	2.222(7)	N(2)-N(4)-Cu(1)#1	125.3(5)
N(5)-Cu(1)#3	1.988(6)	C(1)-N(3)-Cu(1)#2	128.6(5)
Cu(1)-N(1)	2.044(6)	N(5)-N(3)-Cu(1)#2	123.9(4)
Cu(1)-N(2)	2.053(6)	N(3)-N(5)-Cu(1)#3	134.2(5)
Cu(1)-N(3)#5	2.222(7)	N(5)#4-Cu(1)-N(1)	92.4(2)
N(4)#1-Cu(1)-N(1)	164.8(3)	N(5)#4-Cu(1)-N(2)	160.1(3)
N(5)#4-Cu(1)-N(3)#5	101.6(2)	N(1)-Cu(1)-N(2)	80.6(3)

Symmetry transformations used to generate equivalent atoms:

#1 -x,-y+2,-z+1; #2 -x+1/2,y-1/2,-z+1/2; #3 x-1/2,-y+3/2,z-1/2; #4 x+1/2,-y+3/2,z+1/2; #5 -x+1/2,y+1/2,-z+1/2.

Complex **2**

Cu(1)-N(2)	1.981(4)	N(2)-Cu(1)-N(2)#1	180.0(3)
Cu(1)-N(1)	2.004(4)	N(2)-Cu(1)-N(1)	81.16(15)
Cu(1)-O(1)	2.583(4)	N(2)#1-Cu(1)-N(1)	98.84(15)
Cu(1)-N(2)#1	1.981(4)	N(1)-Cu(1)-N(1)#1	180.000(1)
Cu(1)-N(1)#1	2.004(4)	N(2)-Cu(1)-O(1)	90.33(14)
N(2)#1-Cu(1)-O(1)	89.67(14)	N(1)-Cu(1)-O(1)	86.94(14)
N(1)#1-Cu(1)-O(1)	93.06(14)	N(3)-N(2)-Cu(1)	138.4(3)

Symmetry transformations used to generate equivalent atoms: #1 -x+1,-y+1,-z+1.

Complex **3**

Cu(1)-N(3)#1	2.005(11)	N(3)#1-Cu(1)-N(1)	114.9(4)
Cu(1)-N(2)#2	2.025(11)	N(3)#1-Cu(1)-N(2)#2	110.3(4)
Cu(1)-N(5)#3	2.101(11)	N(2)#2-Cu(1)-N(1)	102.6(4)
Cu(1)-N(1)	2.079(10)	N(3)#1-Cu(1)-N(5)#3	113.1(4)
N(2)-Cu(1)#4	2.025(11)	N(2)#2-Cu(1)-N(5)#3	115.3(5)
N(3)-Cu(1)#5	2.005(11)	N(1)-Cu(1)-N(5)#3	99.9(4)
N(1)-N(2)-Cu(1)#4	124.1(8)	C(1)-N(3)-Cu(1)#5	135.0(9)

Symmetry transformations used to generate equivalent atoms:

#1 -x+1,y-1/2,-z+3/2; #2 x,-y+1/2,z-1/2; #3 -x+1,-y+1,-z+1; #4 x,-y+1/2,z+1/2; #5 -x+1,y+1/2,-z+3/2.

Table S3. Hydrogen-bonding interactions for **2** and **3**.

	d(D-H···A) [Å]	**d(D-H)** [Å]	**d(H···A)** [Å]	**D(D···A)** [Å]	**<(DHA)** [°]
	O(1)-H(3)···N(4)	0.66	2.54	2.955	123.6
	O(1)-H(3)···N(5)	0.66	2.31	2.901	150.5
2	N(7)-H(1)···N(4)	0.75	2.63	3.016	113.6
	N(7)-H(1)···O(1)	0.75	2.15	2.865	159.4
	O(1)-H(4)···N(6)	0.86	2.09	2.897	155.4
3	N(6)-H(6A)···N(7)	0.860	1.981	2.831	169.8

4. Thermal decomposition

The DSC curves under the linear heating rate of 5 $^{o}C \cdot min^{-1}$ with nitrogen atmosphere are shown in Figure S6 to demonstrate the thermal decomposition processes of complexes **1**, **2** and **3**.

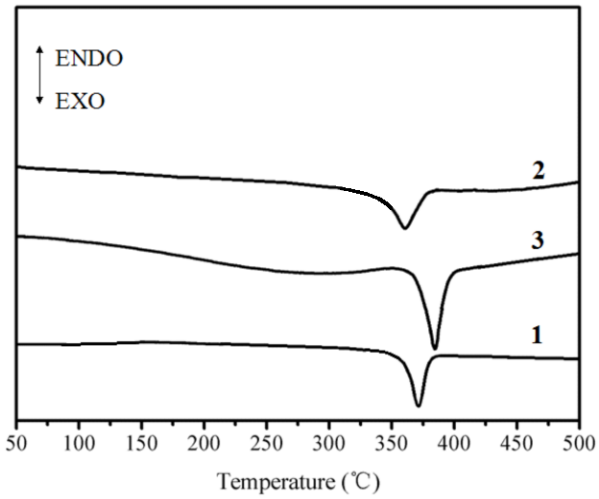

Figure S6. DSC curves of **1**, **2** and **3**.

As shown in Figure S6, for complex **1**, the DSC curve shows that only one intense decomposition process from 345 ^{o}C to 390 ^{o}C with a peak temperature of 370 ^{o}C. For **2**, there is one exothermic process occurs at 325 ^{o}C, ends at 387 ^{o}C with a peak temperature of 360 ^{o}C. For **3**,

there is one sharp exothermic process occurs at 355 °C, ends at 403 °C with a peak temperature of 383 °C.

As shown in Figure 4, TG curves illustrate that complex **1** undergoes one step of weight loss, which correspond to the exothermic processes in the DSC curve. The weight loss is observed from 345 °C to 405 °C, considering as the release of coordinated water molecules and H_2tztr ligands, and the final product with residue mass percentage of 41.3% is in good agreement with the calculated value of CuO (40.74%). There is one mass-loss stage in the range of 85-392 °C for **2**, which due to the continuous loss of guest water molecules in decomposition process. The weight loss stage occurs from 85 °C to 325 °C with the ratio of 7.7% which is attributed to the loss of guest water molecules (8.3%), and the incredibly small heat release of the water molecule is not emerged in the DSC curve. Then, the weight loss is observed up to 392 °C, considering as the collapse of the main frameworks, which correspond to the exothermic process in the DSC curve, and the final product of Cu with residue mass percentage of 46.5% is in good agreement with the calculated value 45.9%. For **3**, there is one weight loss process which corresponds to only one peak in the DSC curve. The step from 355 °C to 413 °C is considered that the complex completely converts to the product Cu with the residue mass percentage of 50.09% which is in good agreement with the calculated value 49.83%.

5. Heat of detonation

Density functional theory (DFT) is used to calculate the energy of detonation (ΔE_{det}), from which ΔH_{det} is estimated by using a linear correlation equation ($\Delta H_{det} = 1.127\Delta E_{det} + 0.046$, r=0.968). As in Ref. 5, the DFT calculation for energetic MOF was performed with the code DMOl3[6] under 3D periodic boundary conditions employing the Monkhorst–Pack multiple K-point sampling of the Brillouin zone[7] and the Perdew–Becke–Ezerhoff (PBE) exchange-correlation function.[8] The detonation reactions considered for three complexes are described by Equations (1), (2) and (3), the values of ΔE_{det} and ΔH_{det} are showed in Table S4.

$$CuC_6H_8N_{14}O_2 \longrightarrow CuO+6C+2NH_3+6N_2+H_2O \quad (1)$$

$$CuC_3H_3N_7O \longrightarrow Cu+3C+\frac{1}{3}NH_3+\frac{10}{3}N_2+H_2O \quad (2)$$

$$CuC_3H_2N_7 \longrightarrow Cu+3C+\frac{2}{3}NH_3+\frac{19}{6}N_2 \quad (3)$$

Table S4. Calculated parameters used in the detonation reactions for three complexes.

	Complex (hartree)	Cu (hartree)	CuO (hartree)	H_2O (hartree)	N_2 (hartree)	C (hartree)	NH_3 (hartree)	$\triangle E_{det}$ (hartree)	$\triangle E_{det}$ (kcal·g^{-1})	$\triangle H_{det}$ (kcal·g^{-1})	$\triangle H_{det}$ (kcal·cm^{-3})
1	-1346.0753		-272.484	-76.3776	-109.447	-37.738	-56.5045	1.0947	1.8475	2.1281	4.0263
2	-769.7539	-196.1132		-76.3776	-109.447	-37.738	-56.5045	0.3909	1.1322	1.3220	3.0617
3	-694.6837	-196.1132			-109.447	-37.738	-56.5045	1.1046	3.4714	3.9582	9.6382

6. Detonation properties

Detonation properties of three complexes and related compounds are investigated by Kamlet-Jacbos (K-J) equations,[9] following as Equations (4), (5) and (6)

$$D=1.01\Phi^{1/2}(1+1.30\rho) \quad (4)$$

$$P=1.558\Phi\rho^2 \quad (5)$$

$$\Phi=31.68N(MQ)^{1/2} \quad (6)$$

where D is detonation velocity (km·s^{-1}). P is detonation pressure (GPa). N is moles of detonation gases per gram of explosive. M is average molecular weight of the gases. Q is chemical energy of detonation (kcal·g^{-1}). ρ is density of explosive (g·cm^{-3}). The complete detonation reactions are described by Eqs. (1), (2) and (3). The D and P values of three complexes are calculated as 8.18 km·s^{-1} and 30.57 GPa for **1**, 7.92km·s^{-1} and 31.99 GPa for **2**, 10.40 km·s^{-1} and 56.48 GPa for **3**.

7. Sensitivity

Impact sensitivities are determined by Fall Hammer Apparatus. Twenty milligrams of the complexes are compacted to a copper cap under the press of 39.2 MPa and are hit by 2 kg drop hammer, and the calculated values of h_{50} represent the drop height of 50% initiation probability. Friction sensitivities of three complexes are measured by applying a Julius Peter's machine using 20 mg sample.

Electrostatic sensitivities are tested by using an ESD JGY-50 III electric spark tester across a small (5 crystals) sample of the material.

8. Non-isothermal kinetics analysis

In this work, Kissinger's method[10] and Ozawa–Doyle's method[11,12] are employed to determine the apparent activation energy (E) and the pre-exponential factor (A). The Kissinger (Eq. (1)) and Ozawa–Doyle (Eq. (2)) equations are as follows:

$$\ln(\frac{\beta}{T_p^2}) = \ln\frac{AR}{E} - \frac{E}{R}\frac{1}{T_p} \qquad (1)$$

$$\log\beta + \frac{0.4567E}{RT_p} = C \qquad (2)$$

where T_p is the peak temperature (°C); A is the pre-exponential factor (s^{-1}); E is the apparent activation energy ($kJ \cdot mol^{-1}$); R is the gas constant ($J \cdot mol^{-1} \cdot {}^oC^{-1}$); β is the linear heating rate (${}^oC \cdot min^{-1}$) and C is a constant.

Based on the exothermic peak temperatures measured at four different heating rates of 2, 5, 8 and 10 ${}^oC \cdot min^{-1}$, the thermo kinetic parameters of three complexes are calculated. The apparent activation energy E_k and E_o, pre-exponential factor A and linear correlation coefficients R_k and R_o for three complexes are shown in Table S5.

The calculated results using both methods are quite close, which are all in the normal range of kinetic parameters for the thermal decomposition reaction of solid materials.[13] Using the obtained E_a (the average of E_k and E_o) and ln$A$ value, the Arrhenius equations can be expressed as $\ln k = 13.3876\text{-}194.2155\times10^3/RT$ (**1**), $\ln k = 14.384\text{-}202.52\times10^3/RT$ (**2**), $\ln k = 17.45\text{-}246.283\times10^3/RT$ (**3**) for the exothermic processes, which can be used to estimate the rate constants of the initial thermal decomposition processes of three complexes.

Table S5. Peak temperatures of the exothermic stage at different heating rates and kinetic parameters.

β (${}^oC \cdot min^{-1}$)	Peaks temperatures T_p (°C)		
	1	**2**	**3**
2	356.3	347.1	370.0
5	370.8	360.3	382.9
8	379.2	368.5	389.2
10	383.4	372.2	392.1
The calculation results by Kissinger's method E_k ($kJ \cdot mol^{-1}$)	193.893	202.488	247.178
Log A (s^{-1})	13.3876	14.384	17.45
Linear correlation coefficient (R_k)	0.9987	0.9988	0.9987

The calculation results by Ozawa-Doyle's method E_o (kJ·mol^{-1})	194.538	202.552	245.388
Linear correlation coefficient (R_o)	0.9985	0.9985	0.9987

9. References

[1] R. Meyer and J. Köhler (Eds.), *Explosives*, 4th ed. revised and extended, VCH Publishers, New York, 1993, **149**.

[2] R. Meyer and J. Köhler (Eds.), *Explosive*s, 4th ed. revised and extended, VCH Publishers, New York, 1993, **197**.

[3] G. M. Sheldrick, *SHELXS-97*, Program for X-ray Crystal Structure Determination, University of Göttingen, Germany, 1997.

[4] G. M. Sheldrick, *SHELXL-97*, Program for X-ray Crystal Structure Refinement, University of Göttingen, Germany, 1997.

[5] O. S. Bushuyev, P. Brown, A. Maiti, R. H. Gee, G. R. Peterson, B. L. Weeks, L. J. Hope-Weeks, *J. Am. Chem. Soc.* 2012, **134**, 1422-1425.

[6] B. J. Delley, *J. Chem. Phys.* 1990, **92**, 508-17.

[7] H. J. Monkhorst, J. D. Pack, *Phys. Rev. B.,* 1976, **13**, 5188.

[8] J. P. Perdew, K. Burke, M. Ernzerhof, *Phys. Rev. Lett.* 1996, **77**, 3865.

[9] M. J. Kamlet, S. Jacobs, *J. Chem. Phys.*, 2003, **48**, 23-35.

[10] H. E. Kissinger, Reaction kinetics in differential thermal analysis, *Anal. Chem.* 1957, **29**, 1702-1706.

[11] T. Ozawa, A new method of analyzing thermogravimetric data, *Bull. Chem. Soc. Jpn.* 1965, **38**, 1881-1886.

[12] C. D. Doyle, Kinetic analysis of thermogravimetric data, *J. Appl. Polym. Sci.* 1961, **5**, 285-292.

[13] R. Z. Hu, Z. Q. Yang and Y. J. Liang, *Thermochim. Acta.* 1988, **123**, 135-151.